

Modelling and Operation of HVDC Based Power Transmission System

Mohd Liaqat

M.Tech Scholar, Electrical Engineering Department,
Yamuna Institute of Engineering & Technology, Yamunanagar, Haryana, India

ABSTRACT

Submodule overcurrent caused by DC pole-to-pole fault in modular multilevel converter HVDC (MMC-HVDC) system is one of the important research objects about its electrical characteristics. In this paper, the fault mechanism before and after the converter blocked was analyzed respectively and the circuit model for the analysis of submodule overcurrent was explored. The analytic equation for overcurrent calculation was deduced and a detailed analysis was also performed. The changes of submodule overcurrent stress with different circuit parameters were obtained and the key issues were also summed up. The results indicate that the submodule overcurrent is the AC system three-phase short-circuit current superposed the discharging current before the converter blocked, and the submodule overcurrent is the AC system three-phase short-circuit current superposed the valve reactor freewheeling current after the converter blocked. From the computation and simulation results, it is concluded that the analytical method is feasible and its calculation results are comparatively precise.

KEYWORDS: HVDC circuit breakers (CBs), HVDC interrupters, HVDC transmission, HVDC converters, power transmission, switchgear

I. INTRODUCTION

The electrical power grid is one of the most important engineering achievements of the 20th century. The conversion of primary energy to electrical energy allows, through the electrical grid infrastructure, to connect power sources with electrical load devices over long distances. The availability of electrical energy is essential for virtually all aspects of daily life, including the supply of water, heating, food, medical care, transport and economic infrastructure. Stability and reliability of the electrical power grid is therefore critical for the well-being of human society. The power grid in today's form has its origins more than a century ago. During the 1890s the rivalry between two approaches to the transmission of electrical energy, alternating current (AC) and direct current (DC), became known as the War of the Currents [1]. Three phase AC transmission prevailed and has ever since dominated the development of the electrical power grid throughout the world until today. A decisive factor was the convertibility of AC power to high voltage levels using transformers. This greatly reduced the transmission losses compared to DC power, which could at that time not be directly converted to high voltage levels [2]. The development of point-to-point high voltage direct current (HVDC) connections continued, following the basic structure of a pair of AC-DC-converters located at two buses in a surrounding AC grid with a DC link in between. The first commercial HVDC link was installed in 1954 between the Swedish coast and the island of Gotland [3], with converter switches based on mercury arc valves. HVDC gained increased interest from the 1970s onwards, when semiconductor technology became available for the development of new efficient converter systems. Today's HVDC links can be grouped into two categories, according to the converter technology used. Line-commutated converter HVDC use thyristors to perform converter switches, providing one degree of freedom to select the injections at the AC terminals. Voltage-source converter HVDC (VSC-HVDC) use insulated-gate bipolar transistors to perform converter switches, providing two degrees of freedom to select the

injections at the AC terminals [4]. The comparison of AC and DC technology as transmission solution with a given power rating includes economic and operational aspects [4]. From an economic perspective, HVDC connections require a larger investment for the converter systems at the end points of the DC link. However, since the power is transmitted as DC current, no reactive power losses occur in the transmission link. In comparison, AC connections have a smaller investment for the end point connection, but require additional reactive power compensation and cable material, increasing the cost per kilometer. The economic break-even between AC and DC connections occurs at roughly 100 to 200 kilometer, depending on the power rating, the voltage level, the HVDC technology, the location of the connection and the general energy price level [5]. As a result, HVDC connections were often selected as solution for long transmission distances [6], the connection of offshore windfarms [7], islands [8], or coastal links across seas [9]. From an operational perspective, HVDC links have the ability to connect otherwise disconnected asynchronous AC grids. This increases the flexibility to support either AC grid using bi-directional external infeed from the HVDC link [10]. An operational difficulty is the behavior of HVDC links during faults. Unlike AC currents, DC currents have no natural zero crossing and must be forced to zero during the opening of a connection [11]. Further criteria for the selection of AC or DC technology concern social and environmental aspects, such as the requirement to put new transmission links underground. The ongoing development towards a hybrid power grid with both AC and DC components aims at exploiting the advantages of both technologies in order to maximize the efficiency, reliability and flexibility of the future energy infrastructure [12]. A feature of HVDC technology that is little exploited in today's grid operation is its potential as dynamic control device to improve the power system performance during transients. A VSC-HVDC link can independently control the active and reactive power injected into the surrounding AC grid. This increased flexibility is already used

by the network planner quasi-statically to optimize power flows between generation and load centers of the AC network [13]. However, the response time of HVDC converters to changes in the injection references is sufficiently fast to also support the network during critical system transients due to faults, the loss of power system components, inter-area oscillations, or variable injections of renewable energy sources. Dynamic grid controllability becomes more important as the power system operates closer to its security margins and is particularly valuable during stress scenarios. It is typically ensured by control actions at the power grid's synchronous generators through droop controller, automatic voltage regulators (AVR) and power system stabilizers (PSS) [14]. In addition, flexible AC transmission system (FACTS) devices provide adjustable reactive power compensation at selected buses in the AC grid [7]. The potential dynamic grid controllability from HVDC connections relies on temporary adjustments of the converter injections into the AC grid. HVDC can provide both local and global dynamic power system support since they directly affect the power flow between remote areas [11, 12, and 13]. This thesis focuses on HVDC links as power system control devices in the presence of transient phenomena in the surrounding power network. Specifically, it addresses three key aspects of the dynamic operation of HVDC links:

- What are the constraints for the dynamic operation of HVDC links in AC networks?
- How should HVDC links be operated to best support the power system during transients?
- Where should HVDC links be located in a given AC network for best dynamical support?

The context and contributions related to each of these questions are summarized in the following section. Throughout the thesis, unless stated otherwise, the term "HVDC" refers to the voltage source converter type (VSC-HVDC).

The topologies of two converters in the VSC-HVDC system have been studied in [17–21]. The two-level bridge is the simplest circuit configuration and there are several commissioned projects that use this topology [15, 16]. Recent practices have extended the principle to multilevel converters by the use of capacitors and diodes to increase the number of levels. The voltages can be clamped for different levels such as a three-level neutral point clamped voltage source converter [14, 18, 22] and a three-level flying capacitor voltage source converter [19, 21]. These multilevel converters provide improved waveform quality and reduced power losses. In [23] it is stated that the typical losses of the two-level and three-level VSC, operating at 1 pu power, are larger than 3% and between 1% – 2%, respectively. However, due to the increased complexity in converter design with multilevel converters the two-level converter technology is still the most commonly used. To fully exploit the capabilities of the VSC-HVDC proper control algorithms are needed. In a number of papers, such as [18, 22, 24, 25], different control systems of the VSC-HVDC have been analyzed. In [18] an inner current control loop for the use together with a carrier based PWM is presented. The inner current control loop is designed for a digital control implementation and for a dead-beat control of the converter current when the converter is connected to a very strong AC network. A grid-connected VSC using a discrete vector current controller is investigated in [24]. The influences of an incorrect controller tuning and grid voltage harmonics on current frequency responses at an

operating point are also addressed. Moreover, some specific aspects of the VSC-HVDC are also studied in the literature. For instance, an analytical model of the power control terminal of a VSC-HVDC system is also analyzed and presented in [26–28]. The contribution of VSC-HVDC to short circuit currents is investigated in [29]. The inter-area decoupling and local area damping by the VSC-HVDC are studied in [30]. There are also some further possibilities for the improvement of VSC-HVDC. In [31] a static synchronous series compensation (SSSC) is embedded in the VSC-HVDC station to improve the dynamic characteristics of the VSC-HVDC link. One of the attractive applications of the VSC-HVDC is that it can be used to connect a wind farm to an AC grid to solve some potential problems such as voltage flicker [32]. In [33] a technical and economical analysis is presented to evaluate the benefits and drawbacks of grid connected offshore wind farms through a DC link. In [34] the behavior of a VSC-HVDC system is studied, when feeding a weak AC network with power produced from an offshore wind farm (WF) of induction generators. The VSC-HVDC connecting a wind farm to an AC system has also been implemented in some commissioned projects [15, 35, 36]. Two commercial VSC-HVDC transmission systems projects, Gotland are feeding onshore wind power to the AC system. These projects have shown that VSC-HVDC is capable of handling wind power and reacting rapidly enough to counteract voltage variations in an excellent way. In February 2005 the world's first offshore VSC-HVDC transmission was successfully commissioned [36]. Overall, the theoretical investigations and experiences confirm that the VSC-HVDC is a promising concept for connecting large wind farms to AC systems. A multiterminal VSC-HVDC can be an attractive alternative to the conventional AC system. The possible implementation of a multiterminal HVDC system and various aspects related to the multiterminal HVDC system have been studied [37–42]. The reliability of a hybrid multiterminal HVDC sub-transmission system is evaluated in [38]. The ability of the multiterminal VSC-HVDC system to improve power quality and how to deal with DC overvoltages during loss of a converter in the multiterminal VSC-HVDC system is investigated in [43] and [40]. The protection of multiterminal VSC-HVDCs against DC faults is also studied in [44]. In the literature there are some other applications of the VSC-HVDC technology. In [45] a study of SSSI (subsynchronous torsional interaction) related to VSC-HVDC is presented. One DC prototype system has been simulated to investigate the opportunities and challenges in industrial systems [46].

II. MODELLING AND CONTROL STRATEGY OF THE VSC-HVDC

The main circuit of a three-phase AC-DC voltage source converter is shown in Figure 1.

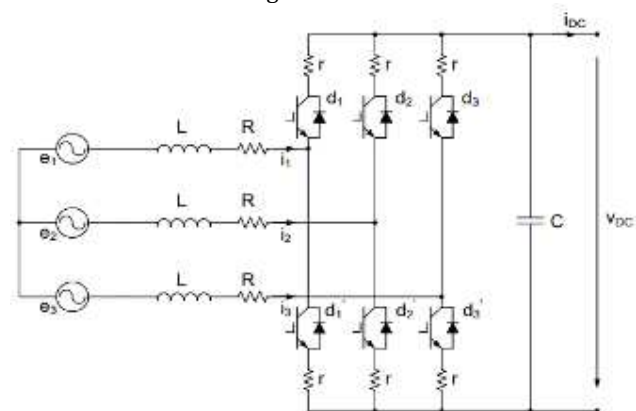


Fig. 1: Circuit diagram of a three-phase VSC

The three-phase mathematical model for a VSC similar to the one presented above was presented in [23] and [24]. If a balanced three-phase system with neutral connection is assumed and neglecting the resistance r of the switches [24], the voltage source converter can be modeled by using equations (4.1) - (4.2):

$$Cd \frac{v_{DC}}{dt} = \sum_{k=1}^3 i_k d_k - i_{DC} \tag{1}$$

$$Ld \frac{i_k}{dt} + Ri_k = e_k - v_{DC} (dk - \frac{1}{3} \sum_{n=1}^3 d_n) \tag{2}$$

Where,

- k - represents the index for the three-phase;
- dk - represents the duty cycle;
- e_k - represents the phase voltage;
- i_k - represents the phase current;
- v_{DC} - represents the DC-link voltage;
- i_{DC} - represents the DC current;
- r - represents the resistance of the switch;
- L - represents the inductance of the phase reactor;
- R - represents the resistance of the phase reactor.

Thus, using equations (1) and (2), the block diagram of a three-phase VSC can be obtained:

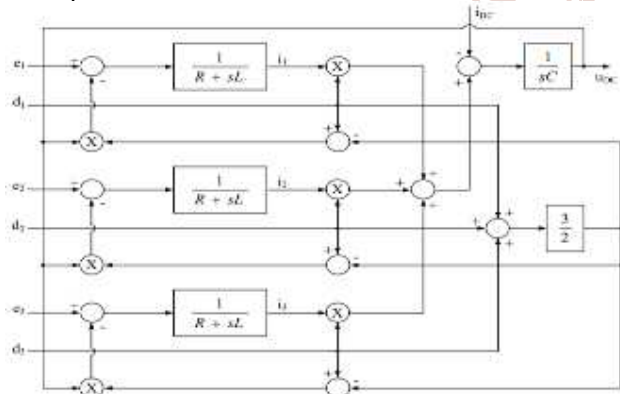


Fig. 2: The block diagram of a three-phase VSC

Based on the three-phase mathematical model of the voltage source converter, the converter's model in the d_q synchronous reference frame can be derived. The model of the VSC in the d_q reference frame will be implemented in Simulink and used for further study-cases analysis. In order

to achieve the mathematical model of the VSC in the d_q synchronous reference frame, the orientation of the d_q system, in the complex plane, in respect to the three-phase system, is considered as presented in Figure 3.

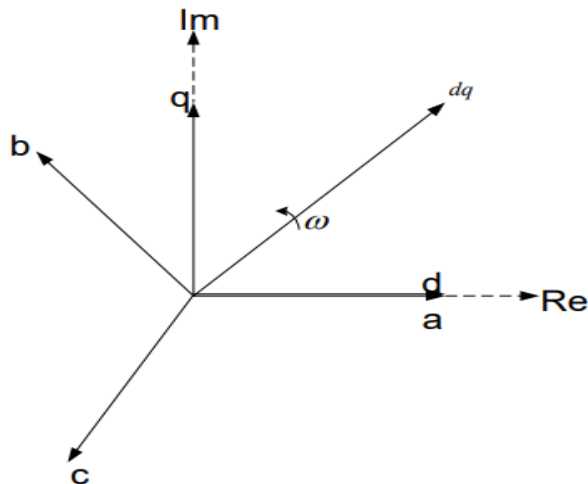


Fig. 3: Orientation of the d_q and three phase systems in the complex plane

DQ transformation is the transformation of coordinates from the three-phase stationary coordinate system to the d - q rotating coordinate system. This transformation is made in two steps:

- A transformation from the three-phase stationary coordinate system to the two-phase, α - β stationary coordinate system and
- A transformation from the α - β stationary coordinate system to the d - q rotating coordinate system.

Clark and Inverse-Clark transformations are used to convert the variables (e.g. phase values of voltages and currents) into stationary α - β reference frame and vice-versa. Similarly, Park and Inverse-Park transformations convert the values from stationary α - β reference frame to synchronously rotating d - q reference frame and vice versa. The reference frames and transformations are shown in Fig 3.

The stationary α -axis is chosen to be aligned with stationary three phase a -axis for simplified analysis. The d - q reference frame is rotating at synchronous speed ω with respect to the stationary frame α - β , and at any instant, the position of d -axis with respect to α -axis is given by $\theta = \omega t$.

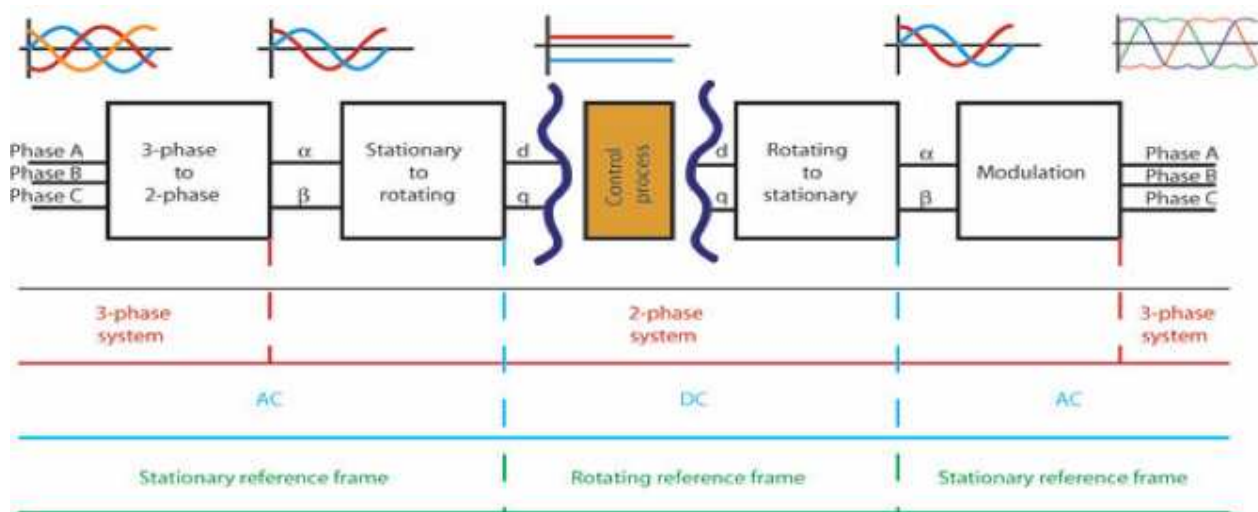


Fig. 4 - Control Stages and respective reference frames

III. FILTER MODEL

The electrical circuit of a three-phase C filter which is to be modeled in this section is shown in Figure 5.

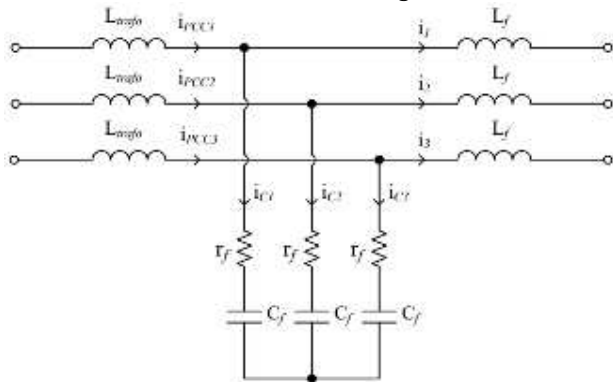


Fig. 5: Circuit diagram of a C filter

The three-phase mathematical model for a C filter similar to the one presented above is discussed in detail in [25]. If the resistance r_f of the capacitor is neglected, the filter can be modeled by using equations (3), (4):

$$C_f \frac{de_k}{dt} = i_{ck} \tag{3}$$

$$i_{ck} = i_{PCCk} - i_k \tag{4}$$

Where,

- k - represents the index for the three-phase;
- e_k - represents the phase voltage;
- i_k - represents the current across filter capacitance;
- i_{PCCk} - represents the phase current at PCC;
- i_{ck} - represents the current flowing in the capacitor;
- C_f - represents the filter's capacitor;
- r_f - represents the internal resistance of the capacitor.

A. GRID MODEL

Usually, a grid model can be developed by using the Thevenin equivalent circuit [26]. The equivalent circuit per phase for the grid model is presented in Figure 4.6, where by an (R-L) equivalent impedance the distribution lines are emulated.

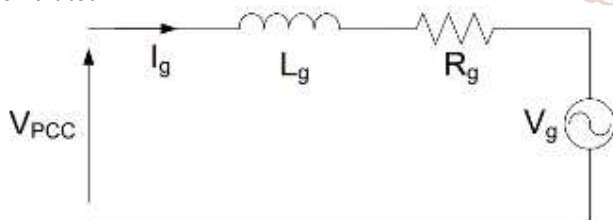


Fig. 6: Thevenin equivalent circuit

B. CONTROL SYSTEM

With classic HVDC the reactive power cannot be controlled independently of the active power. With VSC-HVDC there is an additional degree of freedom. As described in previous chapter, the VSC-HVDC can control the active and reactive power independently. The reactive power can be controlled separately in each converter by the required AC voltage or set manually. The active power flow can be controlled by the DC voltage, the variation of frequency at the AC side or set manually. This means that the active power flow, the reactive power flow, the AC voltage, the DC voltage and the frequency can be controlled when using VSC-HVDC. The control system of the VSC-HVDC is a cascade control system, it typically consists of a faster vector controller. Furthermore, the vector controller is completed by additional controllers which supply the references for the vector controller. Thus, the vector controller will be the inner loop and additional controllers will be the outer loop. In this thesis the additional controllers will be referred to as the outer controllers. The outer controllers include the DC voltage controller, the AC voltage controller, the active power controller, the reactive power controller or the frequency controller. For example, as shown in Fig.7, either side of the link can choose between AC voltage controller and reactive power controller. Obviously not all controllers can be used at the same time. The choice of different kinds of controllers will depend on the application and may require advanced power system studies. For example, the VSC-HVDC can control frequency and AC voltage if the load is a passive system, the VSC-HVDC can control AC voltage and active power flow if the load is an established AC system. However, since the active power flow into the DC link must be balanced, the DC voltage controller is necessary in order to achieve active power balance. Active power out from the DC link must equal the active power into the DC link minus the losses in the DC link. Any difference would result in a rapid change of the DC voltage. The other converter can set any active power value within the limits for the system. In this chapter the vector controller and various outer controllers will be described in detail. Simulation results will be presented in the next chapter.

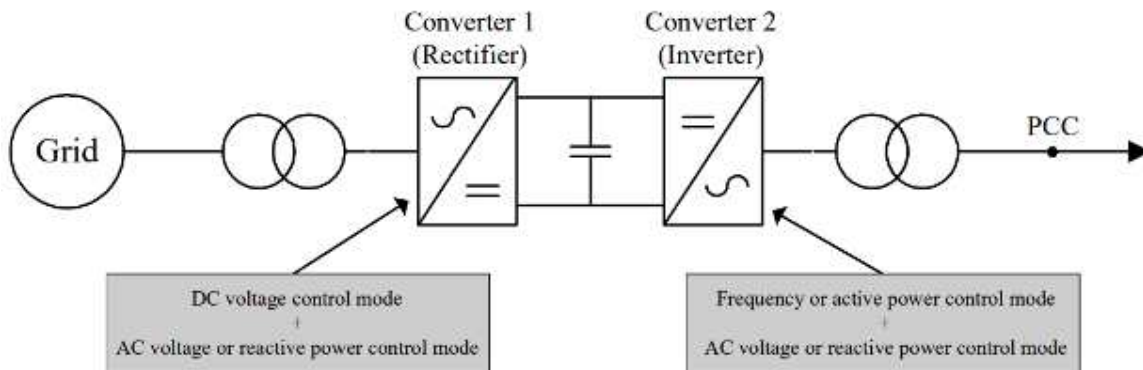


Fig. 7 Overall control structure of the VSC-HVDC

C. VECTOR CONTROLLER

The vector controller is based on the basic relationship of the circuit shown in Fig. 8 and can be implemented in the dq-coordinate system. In order to have a detailed overview of the vector controller, its derivation is presented in this section.

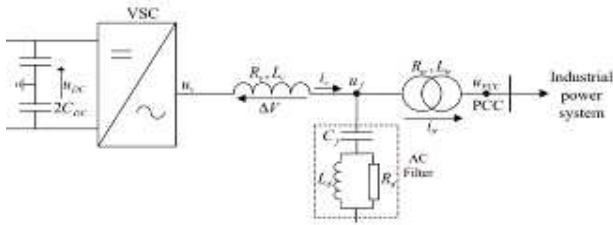


Fig. 8 The inverter station of the VSC-HVDC

From the circuit shown in Fig. 2, the voltage over the transformer, the current through the AC filter and the voltage over the phase reactor can be obtained in the three phase system:

$$u_f^{(abc)}(t) - u_{PCC}^{(abc)} = L_r \frac{d}{dt} i_{tr}^{(abc)}(t) + R_r i_{tr}^{(abc)}(t) \tag{5}$$

$$i_v^{(abc)}(t) - i_{tr}^{(abc)} = C_f \frac{d}{dt} u_f^{(abc)}(t) \tag{6}$$

$$u_v^{(abc)}(t) - u_f^{(abc)} = L_v \frac{d}{dt} i_v^{(abc)}(t) + R_v i_v^{(abc)}(t) \tag{7}$$

D. DC VOLTAGE CONTROLLER

The instantaneous active power $P_f^{(dq)}$ and reactive power $Q_f^{(dq)}$ together with the power P_{rec} transmitted on the DC side of the VSC are expressed as:

$$P_f^{(dq)}(t) = u_f^{(d)} i_v^{(d)}(t) + u_f^{(q)} i_v^{(q)}(t) \tag{8}$$

$$Q_f^{(dq)}(t) = u_f^{(q)} i_v^{(d)}(t) - u_f^{(d)} i_v^{(q)}(t) \tag{9}$$

$$P_{rec}(t) = u_{DC}(t) i_{DC}(t) \tag{10}$$

E. ACTIVE POWER CONTROLLER

A simple method to control the active power is an open-loop controller. The reactive current reference is obtained from (9) as:

$$i_v^{(q)} = \frac{P_f^*}{u_f^q} \tag{11}$$

Where P_f^* is the desired (reference) active power. If an accurate control of the active power is needed, a combination of a feedback loop and an open loop can be used:

$$i_v^{(q)} = \frac{P_f^*}{u_f^q} + (k_{p,Pf} + \frac{k_{I,Pf}}{s})(P_f^* - P_f) \tag{12}$$

Where $k_{p,Pf}$ and $k_{I,Pf}$ are the proportional and integral gains of the active power controller.

IV. SIMULATION RESULTS

The system considered in this thesis is given in Fig.8. The HVDC system consists of two VSCs connected via a dc link. The control of sending end converter (SEC) is done by using dc-voltage control and reactive power control whereas the control of receiving end converter (REC) is done by active and reactive power control.

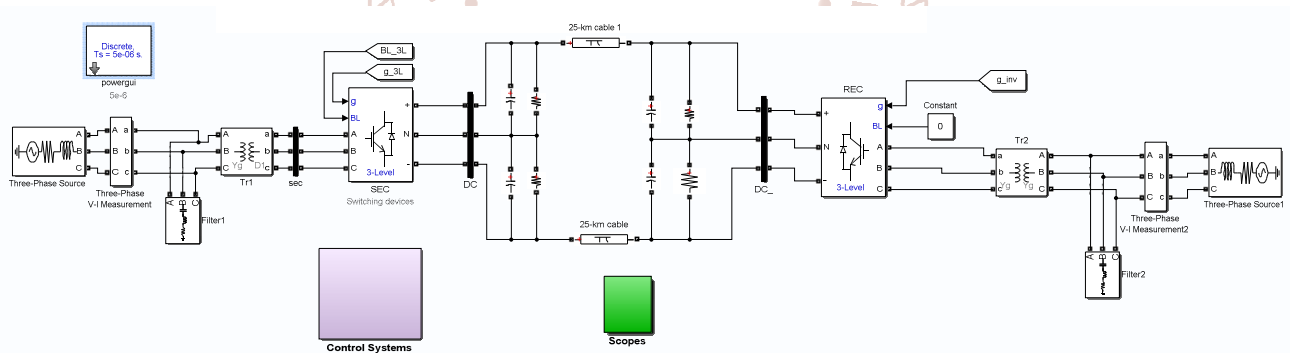


Fig.8 – Test System under consideration:- MATLAB/Simulink

The test system specifications are given in Table 5.1.

Table 5.1 Parameters specifications of test system

Parameter	Speciation
Grid voltage	50 kV
Nominal power	200 MW
Nominal frequency	50 Hz
Sampling time	50 msec
DC link voltage	3000 V
Switching devices	IGBT

Sending end converter (SEC)

Grid voltage and grid current are first converted in to per unit values. DC link voltage which is set at 3000 V is also an input to the SC control system. V_{DC} controller calculates the V_{DC} reference voltage for maintaining the DC link voltage constant and gives signal as I_{dr} reference. Grid voltage and grid current are converted in to d-q axis frame by using abc-

dq transformation. The signals from grid current produces id and iq whereas DC link voltage gives I_{dr} . For producing I_{qr} , grid voltage signal is utilized. The V_d and V_q voltage is compared with actual value of DC link voltage and the error signal is taken as to produce pulses for VSC.

The first study case aims to investigate the steady-state behavior of the VSC-based HVDC transmission system. As discussed in the previous chapter, the outer controllers which are implemented depend on the application. Thus, in this study case the following control loops are considered:

- The offshore converter (which emulates the WPP) controls the active power and the reactive power;
- The onshore converter (which emulates the AC grid) controls the DC voltage and the reactive power.

Before starting the analysis of the behavior of the developed VSC-based HVDC transmission system (plant and control) a

convention of signs should be imposed. Therefore, in all the upcoming results, for both the onshore and offshore terminals the sign "-" indicates that the respective terminal is sending power, while the sign "+" indicates that the respective terminal is receiving power.

In order to analyze the behavior of the developed system, changes in the active and reactive power flow are produced at the onshore terminal and a change of the reference value of the DC voltage is also considered order to improve the performance of the outer DC voltage controller two methods were tested: decreasing of the control response and adding a reference pre-filter. The first method offered good results with a simple implementation and it was finally used.

The d and q components of the measured off shore and onshore currents are plotted in Figure 5.5 and Figure 5.6,

respectively. From these plots it can be noticed that the measured signals are tracking well the reference signals; the overshoot caused by the transients have an acceptable value, while the measured signals are settling fast after the transient ends.

Due to the fact that i_d determines the active power, it can be observed that its reference is changing proportionally with the reference of the active power (see Figure 9). On the other hand, because i_q is directly related with the reactive power, its reference is changing according to the changes in the reactive power flow.

Moreover, because the d and q components of the current are cross-coupled each change in the waveform of a component will cause a small transient in the waveform of other component.

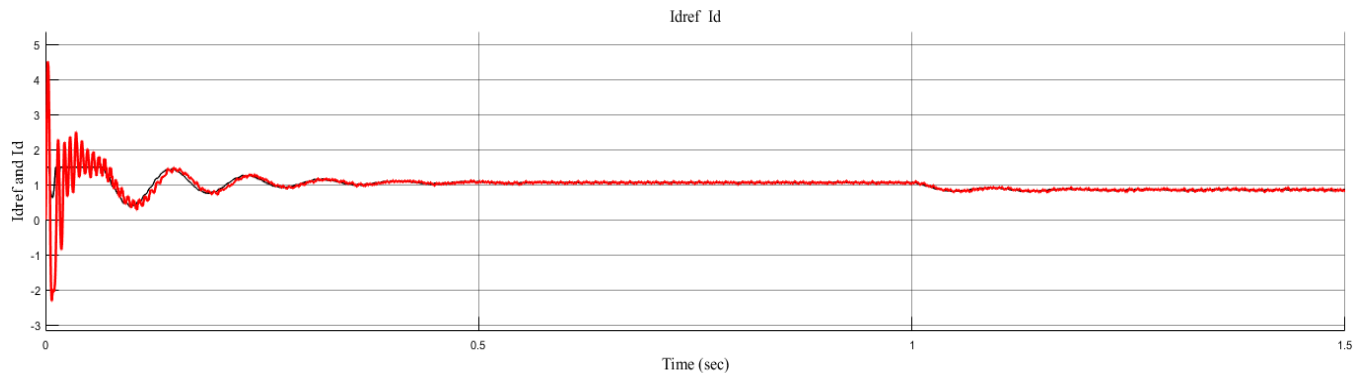


Fig 9 I_{dref} and I_d current variations

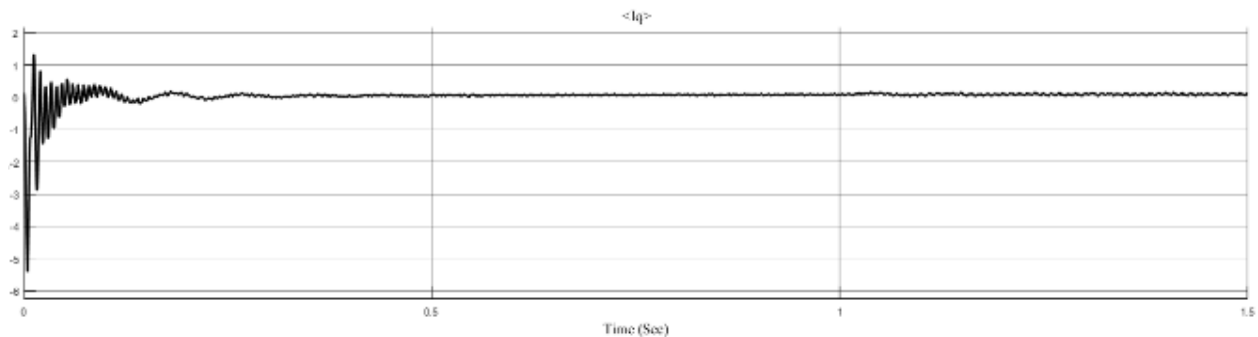


Fig 10 I_{qref} current variations

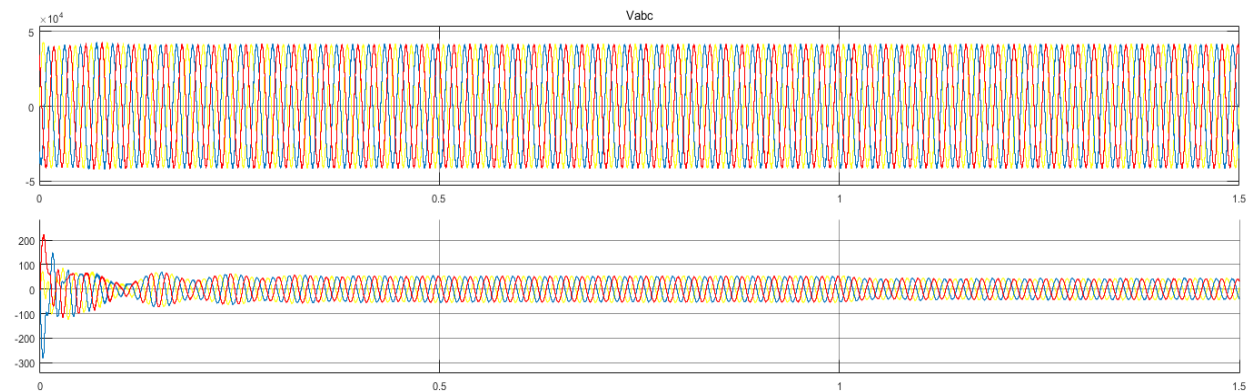


Fig. 11 Three phase grid voltage and grid current

Fig 11 shows the three phase grid voltage and grid current waveform. From the figures it can be seen that as the three phase current is varied at time interval 1 second, the I_{dref} current is also varied accordingly. Which further helps in maintaining I_d current following the I_{dref} current. As a result there is no variation in the three phase voltage waveform. The pu rms value of the grid voltage is shown in Fig. 12.

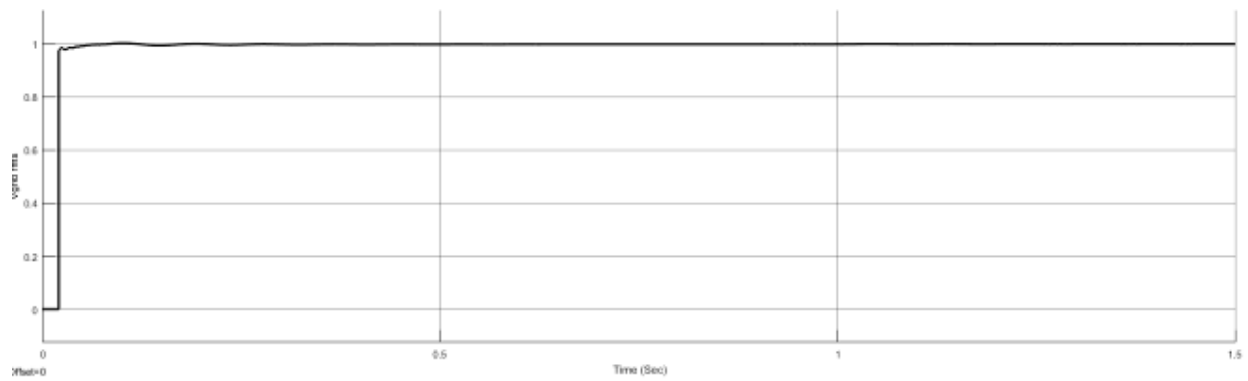


Fig. 12 pu rms value of the grid voltage

Fig 13 shows the voltages for the SEC to the HVDC line. The sum of these two voltages i.e Positive-Neutral and N-Negative is total DC link voltage. This voltage decides the stability of the system. Fig 5.10 shows the resultant DC link voltage of the SEC. Moreover, through this study case the independent control of reactive power at each terminal was verified. The DC voltage controller had shown a good behavior, regulating the DC-link voltage to its reference value, whatever changes in the active power ow were considered

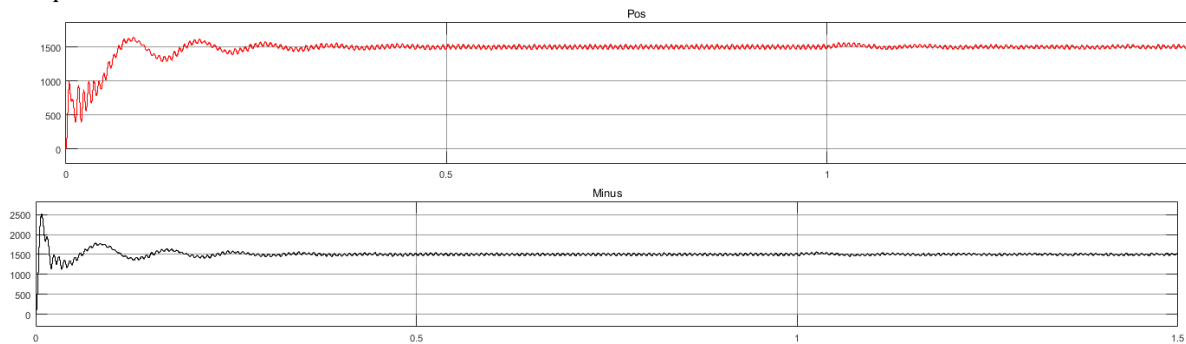


Fig. 13 Positive-Neutral and Neutral-Negative terminal voltage of SEC

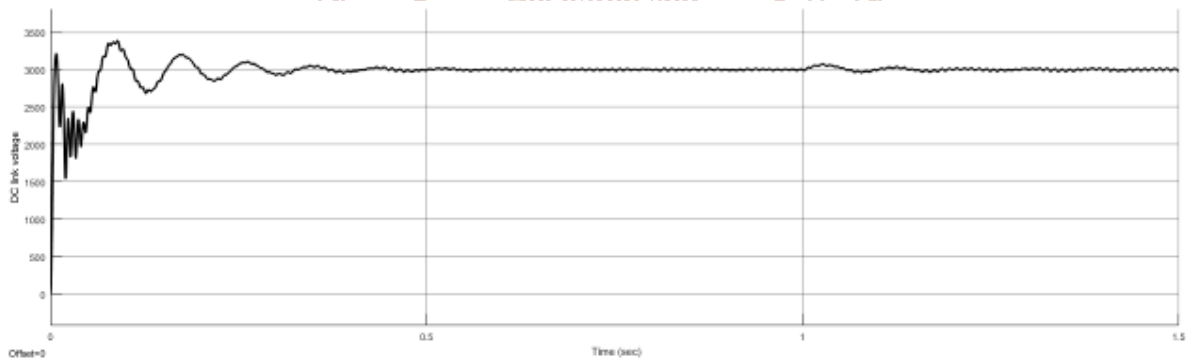


Fig. 5.10 DC link voltage of SEC

The measured active power at both terminals and the power delivered by the grid are plotted. As it can be observed, the value of the measured active power at the sending end terminal is varied at time interval 1 second. The simulated VSC-HVDC system no losses have been considered.

V. CONCLUSIONS

The main topic of this project was to investigate and to analyze the behavior of the VSC- based HVDC transmission system. The current project was structured into six chapters which will be briefly presented in the followings.

The first chapter represents an introduction to the project. This chapter contains a short background, the problem formulation and also the objectives of this project are stated in this section.

The second chapter could be seen as an overview of the literature review of the previous works conducted by various researchers.

The third chapter of the project dealt with the modeling of a simple VSC-based HVDC transmission systems. Here, the mathematical models of the main components (VSC, filter and grid) were presented. Since the control was implemented in the dq synchronous reference frame, the model of the VSC and filter were also developed in the same reference frame.

The next chapter was focused on the design of the control system of the VSC-based HVDC transmission system. In the beginning, an overview of the applicable control loops was realized. As it was shown, all the control strategies have at their bottom level a fast inner current control loop. The

slower outer control loops can regulate various parameters, such as: DC voltage, AC voltage, active power, reactive power and/or frequency. Depending on the application and on the imposed requirements, one or more of this control loops can be used to control the converter.

The fifth chapter was dedicated to the analysis of the steady-state behavior of the VSC-HVDC system.

REFERENCES

- [1] ABB, Power Systems – HVDC. HVDC light - It's time to connect., 2018. Report from www.abb.com.
- [2] R. Adapa. High-wire act: Hvdc technology: The state of the art. Power and Energy Magazine, IEEE, 10(6):18–29, 2012.
- [3] M.E. Aboul-Ela, A.A. Sallam, J.D. McCalley, and A.A. Fouad. Damping controller design for power system oscillations using global signals. IEEE Transactions on Power Systems, 11(2):767–773, May 1996.
- [4] U. Axelsson, A. Holm, C. Liljegren, K. Eriksson, and L. Weimers. Gotland hvdc light transmission - world's first commercial small scale dc transmission. In CIREC Conference, Nice, France, volume 32, 1999.
- [5] G. Andersson. Power System Dynamics and Control. ETH Zurich, 2013.
- [6] F. Borrelli, A. Bemporad, and M. Morari. Predictive control for linear and hybrid systems. In preparation, draft at <http://www.mpc.berkeley.edu>, 2013.
- [7] O. Krishan and Sathans, "Design and Techno-Economic Analysis of a HRES in a Rural Village," Procedia Comput. Sci., 6th International Conference on Smart Computing and Communications, ICSCC 2017, 7-8 December 2017, Kurukshehra, India vol. 125, pp. 321–328, 2018.
- [8] O. Krishan and Sathans, "Frequency regulation in a standalone wind-diesel hybrid power system using pitch-angle controller," in Proceedings of the 10th INDIACOM; 2016 3rd International Conference on Computing for Sustainable Global Development, INDIACOM 2016, 2016.
- [9] S. Boyd, L. El Ghaoui, E. Feron, and V. Balakrishnan. Linear Matrix Inequalities in System and Control Theory, volume 15 of Studies in Applied Mathematics. SIAM, Philadelphia, PA, June 1994.
- [10] M. Balabin, K. Görner, Y. Li, I. Naumkin, and C. Rehtanz. Evaluation of pmu performance during transients. In Power System Technology (POWERCON), 2010 International Conference on, 2010
- [11] C.D. Barker and N.M. Kirby. Reactive power loading of components within a modular multi-level hvdc vsc converter. In Electrical Power and Energy Conference (EPEC), 2011 IEEE, pages 86–90. IEEE, 2011.
- [12] S. Cole, J. Beerten, and R. Belmans. Generalized Dynamic VSC MTDC Model for Power System Stability Studies. IEEE Transactions on Power Systems, 25(3):1655–1662, August 2010.
- [13] L. Cai and I. Erlich. Simultaneous coordinated tuning of pss and facts damping controllers in large power systems. Power Systems, IEEE Transactions on, 20(1):294–300, Feb 2005.
- [14] E. Koldby and M. Hyttinen, "Challenges on the road to an offshore HVDC grid," presented at the Nordic Wind Power Conf., Bornholm, Denmark, Sep. 10–11, 2009
- [15] L. Tang and B.-T. Ooi, "Protection of VSC-multi-terminal HVDC against DC faults," in Proc. IEEE 33rd Annu. Power Electronics Specialists Conf., 2002, vol. 2, pp. 719–724.
- [16] O. Krishan and Sathans, "Optimum sizing and economical assessment of grid integrated hybrid system for a rural village: A case study," in 1st IEEE International Conference on Power Electronics, Intelligent Control and Energy Systems, ICPEICES 2016, 2017.
- [17] O. Krishan and S. Suhag, "An updated review of energy storage systems: Classification and applications in distributed generation power systems incorporating renewable energy resources," Int. J. Energy Res., no. October, pp. 1–40, Nov. 2018.
- [18] S. Allebrod, R. Hamerski, and R. Marquardt, "New transformerless, scalable modular multilevel converters for HVDC-transmission," in Proc. IEEE Power Electronics Specialists Conf., Jun. 2008, pp. 174–179.
- [19] H. Huang, "Multilevel voltage-source converters for HVDC and FACTS application," in CIGRE SC B4 Bergen Colloq., 2009, p. paper 401
- [20] B. Jacobson, P. Kalsson, G. Asplund, L. Harnefors, and T. Jonsson, "VSC-HVDC transmission with cascaded two-level converters," in CIGRE Session, 2010, pp. B4–B110.
- [21] D. Trainer, C. Davidson, C. Oates, N. MacLeod, D. Critchley, and R. Crookes, "A new hybrid voltage-source converter for HVDC power transmission," in CIGRE Session, 2010, pp. B4–B111
- [22] A. Li, Z. Cai, Q. Sun, X. Li, D. Ren, and Z. Yang, "Study on the dynamic performance characteristics of HVDC control and protections for the HVDC line fault," in Proc. IEEE Power Energy Soc. Gen. Meeting, July 2009, pp. 1–5.